VOL. 10, NO 22, DECEMBER, 2015 ISSN 1819-6608
ARPN Journal of Engineering and Applied Sciences

www.arpnjournals.com

EFFECT OF WELLBORE STORAGE ON THE VERTICAL WELL PRESSURE BEHAVIOR WITH THRESHOLD PRESSURE GRADIENT IN LOW PERMEABILITY RESERVOIRS

Yu Long Zhao[1], Freddy Humberto Escobar[2], Ahmad Jamili[3], Guiber Olaya-Marin[2] and Alfredo Ghisays-Ruiz[4]
[1]State Key Laboratory of Oil and Gas Reservoir Geology and Exploitation, Southwest Petroleum University, Xindu Street, xindu district, Chendu, Sichuan, P. R. China
[2]Universidad Surcolombiana/CENIGAA, Avenida Pastrana - Cra 1, Neiva, Huila, Colombia
[3]The University of Oklahoma, Boyd St. SEC Rm. Norman, OK, USA
[4]Universidad del Atlantico, Fac. de Ciencias Básicas. antigua vía Puerto Colombia, Barranquilla, Atlantico, Colombia
E-Mail: fescobar@usco.edu.co

ABSTRACT

An additional pressure gradient is needed in certain low permeability oil formations to enable fluid flow to overcome viscous forces. That minimum pressure gradient has been referred to as the threshold pressure gradient; TPG. This effect is accentuated with the presence of wellbore storage effects. A new model involving wellbore storage effects is developed and presented here along an interpretation technique so the TPG can be easily and accurately estimated from transient pressure analysis and it was successfully tested by means of a synthetic test.

Keywords: *TDS* technique, pressure transient analysis, vertical wells, wellbore storage.

1. INTRODUCTION

Additional pressure gradient required in low permeability reservoirs for a fluid to flow was first reported by Raymond and Philip (1963). A couple of researches were later introduced; however, it is worth to mention an empirical approach given by Prada and Civan (1999) to estimate its value. The next work was presented by Owayed and Tiab (2008) who provided an analytical solution and an interpretation technique of the flow of a slightly compressible Bingham fluid. Later on, Lu and Ghedan (2011) introduced an analytical solution for the pressure behavior of vertical wells in low permeability reservoirs under the influence of TPG. They conducted well test data interpretation by conventional analysis. Lu (2012) included the effect of TPG on pressure tests in uniform-flux hydraulically fractured vertical wells.

An analytical solution for the horizontal well transient pressure behavior of a naturally-fractured reservoir with the effect of TPG was presented by Zhao *et al*. (2013). This model was then used by Escobar *et al*. (2014) to formulate an interpretation methodology based upon *TDS* technique, Tiab (1993).

The latest work on this subject was published by Escobar *et al*. (2015) who provided a practical interpretation technique for the determination of the TPG in uniform-flux vertical fractured wells. Since fractured wells are assumed to be tested with downhole shut-in devices, the wellbore storage effects were excluded from their analysis but they mentioned that when wellbore storage increases so does the pressure drop.

Zhao *et al.* (2013), Escobar *et al*. (2014) and Escobar *et al*. (2015) observed the effect of the threshold pressure gradient by an upwards deviation of the pressure derivative during radial flow regime. A similar situation is observed in the present work where the impact is also seen on the radial flow regime. This situation is expected to take place since the radial flow in a horizontal well is the same as the radial flow in a vertical well.

In this work, a new mathematical model is presented to understand the well pressure behavior in vertical wells in homogeneous reservoirs with the influence of the threshold pressure gradient including wellbore storage and skin effects. It was observed that wellbore storage effects increase the pressure drop and alters the pressure derivative behavior so the formulation presented by Escobar *et al.* (2015) fails to produce accurate values when the wellbore storage coefficient becomes significant. A practical interpretation technique that follows the *TDS* philosophy was introduced here, so the TPG can be easily and accurately calculated. It was demonstrated with a simulated example.

2. MATHEMATICAL FORMULATION

2.1. Modeling

The governing diffusivity equation along with its initial and boundary conditions are presented below:

$$\frac{1}{r_D}\frac{\partial}{\partial r_D}\left(r_D\frac{\partial P_D}{\partial r_D}\right)+\frac{\lambda_D}{r_D}=\frac{\partial P_D}{\partial t_D} \quad (1)$$

Initial condition:

$$P_D\left(r_D,0\right)=0 \quad (2)$$

Inner boundary condition:

$$\left.\frac{\partial P_D}{\partial r_D}\right|_{r_D=1} = -1 \tag{3}$$

Outer boundary condition:

$$P_D\left(r_D \to \infty, t_D\right) = 0 \tag{4}$$

Bottom-hole pressure:

$$P_{wD} = P_D\big|_{(r_D=1)} \tag{5}$$

The Laplace domain solution is given by:

$$\bar{P}_D(\ell) = \frac{(1+d)K_0\left(\sqrt{\ell}r_D\right)}{\ell\left[\sqrt{\ell}K_1\left(\sqrt{\ell}\right)+\ell K_0\left(\sqrt{\ell}\right)\right]} + \int_1^{\infty} G\left(r_D,\tau\right)d\tau \tag{6}$$

where;

$$d = \lambda_D + \frac{\pi\lambda_D}{2} I_1\left(\sqrt{\ell}\right) - \frac{\pi\lambda_D}{2\sqrt{\ell}}\ell I_0\left(\sqrt{\ell}\right) \tag{7}$$

and,

$$G\left(r_D,\tau\right) = \begin{cases} \dfrac{\lambda_D}{\ell}K_0(r_D\sqrt{\ell})I_0(\tau\sqrt{\ell}), & 1<\tau<r_D \\ \dfrac{\lambda_D}{\ell}K_0(\tau\sqrt{\ell})I_0(r_D\sqrt{\ell}), & r_D<\tau<\infty \end{cases} \tag{8}$$

When the dimensionless radius, r_D, is set to 1, the bottom-hole pressure can be obtained as follows:

$$\tilde{P}_{wD}(\ell) = \frac{(1+d)K_0(\sqrt{\ell})}{\ell\left[\sqrt{\ell}K_1(\sqrt{\ell})+\ell K_0(\sqrt{\ell})\right]} + \frac{\pi\lambda_D}{2\ell\sqrt{\ell}} I_0(\sqrt{\ell}) \tag{9}$$

Including wellbore storage and skin effects:

$$\bar{P}_{wD}(\ell) = \frac{\ell\tilde{P}_{wD}(\ell)+s}{\ell+C_D\ell^2(\ell\tilde{P}_{wD}+s)} \tag{10}$$

2.2. Dimensionless quantities

The dimensionless quantities considered in this study are given below.

$$t_D = \frac{0.0002637kt}{\phi\mu c_t r_w^2} \tag{11}$$

$$P_D = \frac{kh\Delta P}{141.2q\mu B} \tag{12}$$

$$t_D * P_D' = \frac{kh(t*\Delta P')}{141.2q\mu B} \tag{13}$$

$$PG_D = \frac{kr_w h(PG)}{141.2q\mu B} \tag{14}$$

$$C_D = \frac{0.894C}{\phi c_t h r_w^2} \tag{15}$$

2.2. Pressure and pressure derivative behaviors

Figure-1 shows different pressure scenarios obtained with Equation (10) for different dimensionless pressure gradient values expected to occur in field situations under constant wellbore storage conditions. Figure-2 shows pressure derivative values for the same mentioned considerations. As expected the early-time pressure data is governed only by wellbore storage; then, a unit-slope line is observed in both pressure and pressure derivative. Radial flow regime follows a transition period. As remarked by Escobar *et al*. (2015) both pressure derivative during radial flow regime deviates upwards from the horizontal line (with TPG ≈ 0) making it difficult to obtain reservoir permeability if both TPG and wellbore storage values mask the radial flow regime. Both pressure and pressure derivative become parallel to each other with a slope of one half during late radial flow regime.

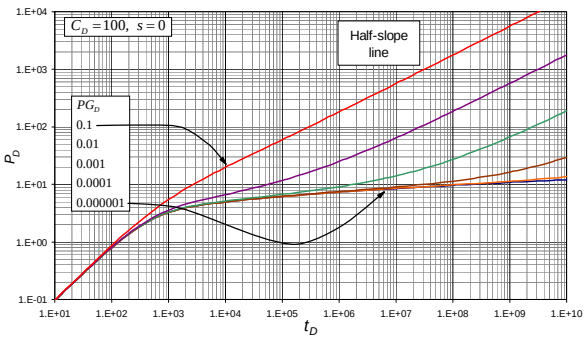

Figure-1. Dimensionless pressure vs. time for different dimensionless pressure gradient values and constant dimensionless wellbore storage coefficient for a vertical well in an infinite homogeneous reservoir.

Effect of wellbore storage on pressure and pressure derivative responses for a given dimensionless pressure gradient is shown in Figure-3. As warned by Escobar *et al*. (2015), the wellbore storage impacts the pressure and pressure derivative behavior by shifting upward the pressure derivative as dimensionless wellbore storage increases. It means the effect of the TPG is shown earlier during radial flow regime as the wellbore storage coefficient increases. Also, the pressure drop, dotted

curves in Figure-4, increases its value as wellbore storage increases indicating an increase in skin factor due to the increase of wellbore storage.

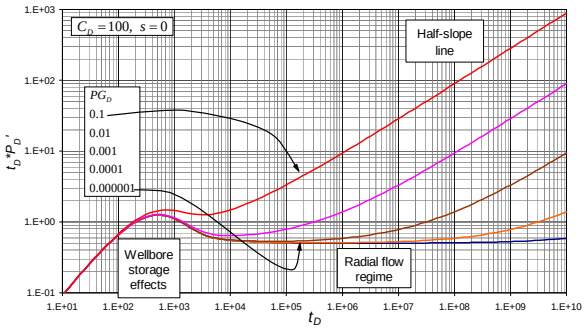

Figure-2. Dimensionless pressure derivative vs. time different dimensionless pressure gradient values and constant dimensionless wellbore storage coefficient for a vertical well in an infinite homogeneous reservoir.

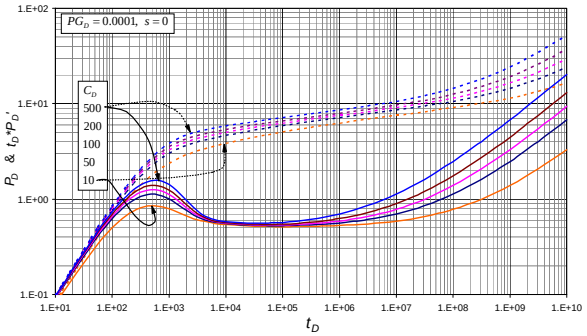

Figure-3. Dimensionless pressure and pressure derivative vs. time for different dimensionless wellbore storage coefficients and a constant pressure gradient.

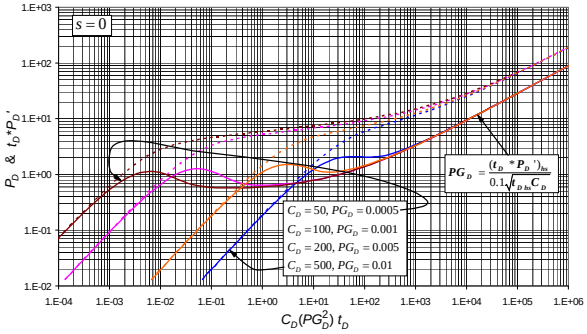

Figure-4. Dimensionless unified behaviour.

2.3. Well pressure data interpretation

Besides providing the model and solution, the other objective of this paper is to provide a practical methodology following the *TDS* technique philosophy, Tiab (1993), for interpretation of well test pressure data under the effect of threshold pressure gradient with the presence of significant wellbore storage conditions. If these conditions are negligible, the methodology presented by Escobar *et al*. (2015) for fractured vertical wells may work for unfractured wells.

Tiab (1993) demonstrated that permeability and skin factor can be obtained from data obtained during radial flow regime;

$$k = \frac{70.6 q \mu B}{h (t * \Delta P')_r} \tag{16}$$

$$s = 0.5\left(\frac{\Delta P_r}{(t * \Delta P')_r} - \ln\left[\frac{k\, t_r}{\phi \mu c_t r_w^2} \right] + 7.43 \right) \tag{17}$$

Since the TPG, see Figure-2, mainly affects the radial flow regime, no effect may be expected at earlier times. Then, in cases when the radial flow is masked by the combined effects of TPG and wellbore storage, the empirical relationships developed by Tiab (1993) can be used to obtain permeability and skin factor from the maximum point taking place at early time:

$$k = \left(\frac{70.6 q \mu B}{h} \right) \frac{1}{(0.014879 qB / C) t_x - (t * \Delta P')_x} \tag{18}$$

$$s = 0.921 \left(\frac{(t * \Delta P)_x}{(t * \Delta P)_i} \right)^{1.1} - 0.5 \ln\left(\frac{0.8935 C}{\phi h c_t r_w^2} \right) \tag{19}$$

It is obtained from Equation (16):

$$(t * \Delta P')_i = (t * \Delta P')_r = \frac{70.6 q \mu B}{hk} \tag{20}$$

For the estimation of the wellbore storage coefficient, Tiab (1993) also presented the following expressions:

$$C = \frac{qB}{24} \frac{t_N}{\Delta P_N} = \frac{qB}{24} \frac{t_N}{(t * \Delta P')_N} \tag{21}$$

Once permeability is known, next step is to determine the dimensionless pressure gradient. For that purpose, the effect of this parameter is unified by multiplying the dimensionless time by the dimensionless pressure gradient to a power of two and by the dimensionless wellbore storage coefficient as given in Figure-4. Both pressure and pressure derivative display a

straight line behavior with a slope of one half (*hs*) which is governed by:

$$PG_D = \frac{(t_D * P_D')_{hs}}{0.1\sqrt{t_{D\,hs} C_D}} \quad (22)$$

Replacing the dimensionless parameters given by Equations (11), (13) and (15) into Equation (22) leads to:

$$PG_D = \frac{4.6126\phi c_t r_w^2 (t*\Delta P')_{hs}}{qB}\sqrt{\frac{h^3 k}{\mu C t_{hs}}} \quad (23)$$

When the data is too noisy it is recommended to extrapolate the linear trend and read the value of the pressure derivative at the time of 1 hour. In such case Equation (23) becomes:

$$PG_D = \frac{4.6126\phi c_t r_w^2 (t*\Delta P')_{hs1}}{qB}\sqrt{\frac{h^3 k}{\mu C}} \quad (24)$$

During unmasked radial flow regime, the dimensionless pressure derivative takes the value of one half. Then, replacing this into Equation (22) will yield:

$$PG_D = 325.6463\phi c_t r_w^2 \sqrt{\frac{\mu h}{k C t_{rhsi}}} \quad (25)$$

3. DETAILED SYNTHETIC EXAMPLE

Pressure data is given in Table-1. Also, the pressure drop and pressure derivative versus time log-log plot for a simulated drawdown is provided in Figure-5. The input data for the simulation is given as follows:

q = 30 BPD	B = 1.1 rb/STB
μ = 2 cp	c_t = 1x10^{-5} psi^{-1}
h = 50 ft	k = 12 md
ϕ = 5 %	C = 0.000252 bbl/psi
PG_D = 0.0001	s = 0
r_w = 0.3 ft	

Solution. The following information was read from Figures-5,

ΔP_N = 0.637 psi	t_N = 0.00012 hr
t_{hs} = 21238.2 hr	$(t*\Delta P')_{hs}$ =45.46 psi
t_{rhsi} =680 hr	t_x =0.016 hr
$(t*\Delta P')_x$ = 19.51 psi	$(t*\Delta P')_r$ = 8.27 psi

The procedure is outlined as follows:

Step-1. Find the wellbore storage coefficient with Equation (21);

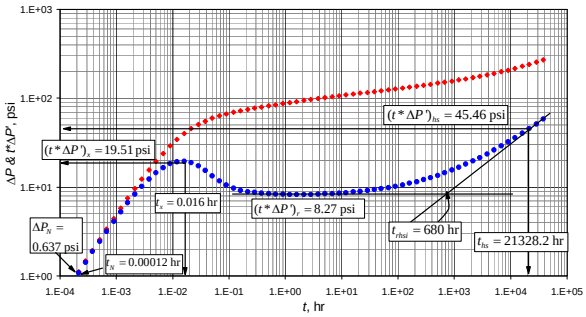

Figure-5. Pressure and pressure derivative data versus time for synthetic example.

$$C = \frac{qB}{24}\frac{t_N}{\Delta P_N} = \frac{(30)(1.1)}{24}\frac{0.00012}{0.637} = 0.000259 \text{ bbl/psi}$$

Step-2. Since it looks that the radial flow is slightly masked then, reservoir permeability can be determined from Equation (16):

$$k = \frac{70.6(30)(2)(1.1)}{50(8.27)} = 12.3 \text{ md}$$

Step-3. For cases when the radial flow is masked by the combined effect of wellbore storage and the TPG, the coordinates of the peak are used to estimate permeability with Equation (18):

$$k = \left(\frac{70.6(30)(2)(1.1)}{50}\right) \frac{1}{\left(0.014879(30)(1.1)/0.000259\right)0.016 - 19.51} \approx 11 \text{ md}$$

Step-4. Find the dimensionless pressure gradient with Equations (23) and (25);

$$PG_D = \frac{4.6126(0.05)(1\times10^{-5})(0.3^2)(45.46)}{(30)(1.1)} \sqrt{\frac{50^3(11)}{2(0.000259)(21238.2)}} = 0.00010087$$

$$PG_D = 325.6463(0.05)(1\times10^{-5})(0.3^2) \sqrt{\frac{2(50)}{11(0.000259)(680)}} = 0.00010528$$

4. COMMENTS ON THE RESULTS

The agreement between the simulated and estimated results in the worked example show that the equations introduced in this study work very well.

Table-1. Pressure drop, pressure derivative and second pressure derivative versus time data.

***t*, hr**	**Δ*P*, psi**	***t**Δ*P'*, psi**
0.00012	0.637	0.621
0.00016	0.839	0.823
0.00021	1.118	1.087
0.00028	1.476	1.429
0.00038	1.942	1.879
0.00051	2.563	2.454
0.00067	3.370	3.184
0.00090	4.411	4.116
0.0012	5.762	5.265
0.0016	7.471	6.663
0.0021	9.630	8.341
0.0028	12.30	10.25
0.0038	15.55	12.36
0.0051	19.43	14.55
0.0067	23.92	16.60
0.0090	28.97	18.30
0.0120	34.39	19.32
0.0160	39.98	19.51
0.0213	45.49	18.79
0.0284	50.67	17.30
0.0379	55.34	15.39
0.0506	59.49	13.45
0.0674	63.12	11.77
0.0899	66.37	10.55
0.12	69.32	9.72
0.16	72.08	9.21
0.21	74.71	8.90
0.28	77.24	8.71
0.38	79.73	8.57
0.51	82.16	8.46
0.67	84.57	8.39
0.90	86.96	8.33
1.20	89.34	8.29
1.60	91.72	8.28
2.13	94.09	8.28
2.84	96.47	8.29
3.79	98.86	8.34
5.06	101.27	8.40
6.74	103.71	8.48
8.99	106.16	8.57
11.99	108.63	8.68
15.99	111.16	8.82
21.33	113.71	8.98
28.44	116.32	9.15
37.94	118.99	9.37
50.57	121.72	9.61
67.43	124.52	9.89
89.93	127.41	10.22
119.94	130.41	10.59
159.93	133.53	11.03
213.28	136.77	11.54
284.41	140.18	12.11
379.41	143.75	12.80
505.69	147.55	13.57
674.35	151.58	14.48
899.32	155.89	15.52
1199.37	160.52	16.71
1599.26	165.52	18.09
2132.82	170.96	19.69
2844.14	176.88	21.53

Table-2. Pressure drop, pressure derivative and second pressure derivative versus time data. Cont.

t, hr	Δ*P*, psi	*t**Δ*P'*, psi
3794.08	183.37	23.67
5056.88	190.53	26.12
6743.46	198.45	28.97
8993.17	207.24	32.24
11993.74	217.06	36.03
15992.61	228.06	40.41
21328.21	240.39	45.46
28441.41	254.29	51.30
37940.84	270.01	58.04

5. CONCLUSIONS

A new model including skin and wellbore storage effects along with its analytical solution to observe transient pressure behavior considering the threshold pressure gradient for a vertical well is introduced.

It was observed that wellbore storage affects adversely the pressure and pressure derivative behavior for a constant threshold gradient pressure. The increase in the wellbore storage coefficient value also causes an increase of the pressure drop.

Extension of the *TDS* technique is given for the case of vertical wells with pressure gradient threshold including wellbore storage and skin effects. Two governing equations for the estimation of this parameter during radial flow regime were developed and successfully tested by a simulated example.

As for the case of horizontal wells and fractured wells, the higher the TPG the more deviated upwards the pressure derivative pseudorradial flow regime from its characteristic horizontal behavior.

This work also includes the estimation of the formation permeability in spite of the absence of the horizontal behavior of the pressure derivative during radial flow regime using the maximum point found during wellbore storage as presented originally by Tiab (1993).

ACKNOWLEDGEMENTS

Authors thank God for all the blessing they have received.

The work financially supported by 973 Program of China under Grant No. 2014CB239205 and the Natural Science Foundation of China (Grant No. 51374181). The authors gratefully thank Universidad Surcolombiana, Universidad del Atlántico, the University of Oklahoma and the State Key Laboratory of Oil and Gas Reservoir Geology and Exploitation in Southwest Petroleum University.

Nomenclature

B	Volumetric factor, rb/Mscf
C	Wellbore storage coefficient, bbl/psi
c_t	System total compressibility, 1/psi
k	Permeability, md
h	Reservoir thickness, ft
P	Pressure, psi
PG	Threshold pressure gradient, psi/ft
PG_D	Dimensionless threshold pressure gradient
r	Radius, ft
s	Mechanical skin factor
t	Time, hr
t_D	Dimensionless time
$t*\Delta P'$	Pressure derivative, psi
t_D*P_D'	Dimensionless pressure derivative

Greeks and symbols

ϕ	Porosity, fraction
μ	Viscosity, cp
ℓ	Laplace parameter

Suffices

D	Dimensionless
hs	Half slope
*hs*1	Half slope read at 1 hr
i	Intersect of radial flow and unit-slope lines
max	Maximum
min	Minimum
rhsi	Intercept between half slope and horizontal radial flow lines
w	Wellbore
wD	Dimensionless well-flowing
x	Maximum point at early time

REFERENCES

Escobar F.H., Zhao Y.L. and Zhang L.H. 2014. Interpretation of Pressure Tests in Horizontal Wells in Homogeneous and Heterogeneous Reservoirs with Threshold Pressure Gradient. Journal of Engineering and Applied Sciences. 9(11): 2220-2228.

Escobar F.H., Zhao Y.L., Pournuk M., Liu Q.G. and Olaya-Marin G. 2015. Interpretation of Pressure Tests in

Uniform-Flux Fractured Vertical Wells with Threshold Pressure Gradient in Low Permeability Reservoirs. Under review in Journal of Engineering and Applied Sciences.

Lu J. and Ghedan S. 2011. Pressure behavior of vertical wells in low-permeability reservoirs with threshold pressure gradient. Special Topics and Reviews in Porous Media. 2(3): 157-169.

Lu J. 2012. Pressure behavior of uniform-flux hydraulically fractured wells in low-permeability reservoirs with threshold pressure gradient. Special Topics and Reviews in Porous Media - An International Journal. 3(4): 307-320.

Owayed J.F. and Tiab. D. 2008. Transient pressure behavior of Bingham non-Newtonian fluids for horizontal wells Journal of Petroleum Science and Engineering. 61. pp. 21-32.

Prada A. and Civan F. 1999. Modification of Darcy's law for the threshold pressure Gradient. Journal of Petroleum Science and Engineering. 22. pp. 237-240.

Raymond J. M. and Philip F. L. 1963. Threshold Gradient for water flow in clay systems Soil Science Society of America Journal. 27. pp. 605-609.

Tiab D. 1993. Analysis of Pressure and Pressure Derivative without Type-Curve Matching: 1- Skin and Wellbore Storage. Journal of Petroleum Science and Engineering. 12: 171-181.

Zhao Y.L., Zhang L.H., Feng W. Zhang B.N and Lis Q.G. 2013. Analysis of horizontal well pressure behavior in fractured low permeability reservoirs with consideration of the threshold pressure gradient. Journal of Geophysics and Engineering. 10, 1-10.